Available online at www.sciencedirect.com
ScienceDirect
Journal of Physics and Chemistry of Solids 67 (2006) 2512–2516
JOURNAL OF PHYSICS AND CHEMISTRY OF SOLIDS
www.elsevier.com/locate/jpcs

Crystal chemistry of layered carbide, $Ti_3(Si_{0.43}Ge_{0.57})C_2$

Hexiong Yang[a,*], B. Manoun[a], R.T. Downs[b], A. Ganguly[c], M.W. Barsoum[c]

[a]*Center for Study of Matter at Extreme Conditions (CeSMEC), Florida International University, VH-140, University Park, Miami, FL 33199, USA*
[b]*Department of Geosciences, University of Arizona, Tucson, AZ 87521, USA*
[c]*Department of Materials Engineering, Drexel University, Philadelphia, PA 19104, USA*

Abstract

The crystal structure of a layered ternary carbide, $Ti_3(Si_{0.43}Ge_{0.57})C_2$, was studied with single-crystal X-ray diffraction. The compound has a hexagonal symmetry with space group $P6_3/mmc$ and unit-cell parameters $a = 3.0823(1)$ Å, $c = 17.7702(6)$ Å, and $V = 146.21(1)$ Å^3. The Si and Ge atoms in the structure occupy the same crystallographic site surrounded by six Ti atoms at an average distance of 2.7219 Å, and the C atoms are octahedrally coordinated by two types of symmetrically distinct Ti atoms, with an average C–Ti distance of 2.1429 Å. The atomic displacement parameters for C and Ti are relatively isotropic, whereas those for A (= 0.43Si + 0.57Ge) are appreciably anisotropic, with U_{11} (= U_{22}) being about three times greater than U_{33}. Compared to Ti_3SiC_2, the substitution of Ge for Si results in an increase in both A–Ti and C–Ti bond distances. An electron density analysis based on the refined structure shows that each A atom is bonded to 6Ti atoms as well as to its 6 nearest neighbor A site atoms, whether the site is occupied by Si or Ge, suggesting that these bond paths may be significantly involved with electron transport properties.

Keywords: C. X-ray diffraction; D. Crystal structure

1. Introduction

Layered carbides and nitrides, or the so-called $M_{n+1}AX_n$ (MAX) phases, where n is 1, 2, or 3, and M represents an early transitional metal, A an A-group element, and X either carbon or/and nitrogen, are a class of materials exhibiting a unique combination of excellent characteristics of both metals and high-performance ceramics. The salient properties of these materials include high-melting temperatures, low density, good thermal and electrical conductivities, high strength and modulus, ease of machinability by conventional tools, exceptional resistance to thermal shock and high-temperature oxidation, damage tolerance and microscale ductility at room temperature [1,2]. Among more than 50 MAX phases synthesized thus far, the compound Ti_3SiC_2 has been a subject of the most extensive investigations.

The general structural features of MAX phases, which all possess the space group $P6_3/mmc$, are that nearly close-packed M layers parallel to (0 0 1) are sandwiched by layers of A-group element, with X atoms occupying the octahedral sites between the former, forming the edge-shared XM_6 octahedral sheets. The principal difference among various structures lies in the number of M layers separating the A layers: it is two, three, and four in the M_2AX, M_3AX_2 and M_4AX_3 compounds, respectively [1]. The current crystal structure models of M_2AX and M_3AX_2 phases were developed from photographic measurements of X-ray diffraction intensities about 40 years ago [3,4]. Since then, only two structures of MAX phases have been investigated with powder neutron and/or X-ray diffraction: Ti_3SiC_2 by Kisi et al. [5] and Barsoum et al. [6], and Ti_4AlN_3 by Rawn et al. [7] and Barsoum et al. [8]. However, due to the difficulty in synthesizing large and good-quality single crystals, no single-crystal X-ray diffraction study has been made yet on any MAX phases, despite its superiority over powder X-ray diffraction in obtaining more precise and detailed structural information, such as electron density distributions, atomic order–disorder, and atomic thermal displacement parameters. As a thorough knowledge of crystal structures of MAX

*Corresponding author. Tel.: +1 305 348 3030; fax: +1 303 348 3070.
E-mail address: yang@fiu.edu (H. Yang).

0022-3697/$ - see front matter © 2006 Elsevier Ltd. All rights reserved.
doi:10.1016/j.jpcs.2006.07.009

phases is crucial for the fundamental understanding of their unique physical and chemical properties and for their industrial applications, we have carried out the first single-crystal X-ray diffraction structure analysis on a MAX phase with the composition $Ti_3(Si_{0.43}Ge_{0.57})C_2$. This work is a part of our effort aiming to understand the chemistry–structure–property relationships of the MAX phases at various conditions. The thermal shock resistance and damage tolerance of $Ti_3(Si_{0.43}Ge_{0.57})C_2$ have been determined by Ganguly et al. [9] and its compressibility up to 53 GPa has been measured by Manoun et al. [10].

2. Experimental procedures

The $Ti_3(Si_{0.43}Ge_{0.57})C_2$ crystal used in this study was prepared from the stoichiometric mixture of Ti, C, SiC, and Ge powders, all of which had purity greater than 99.0 at%, followed by presintering in vacuum-sealed borosilicate glass tubes. The tubes were, in turn, hot-isostatically pressed at 1600 °C for 8 h. The chamber was pressurized with Ar to ~172 MPa. The detailed synthesis procedure was described by Ganguly et al. [9]. Based on optical examination and X-ray diffraction peak profiles, a nearly cube-shaped crystal was selected from the crushed sample and mounted on a Bruker X8 Apex CCD X-ray diffractometer equipped with graphite-monochromatized MoK_α radiation. A hemisphere of three-dimensional X-ray diffraction data was collected at room temperature with frame widths of 0.5° in φ and 20 s counting time per frame. The data were analyzed to locate peaks for the determination of the unit-cell parameters. All reflections were indexed based on a hexagonal unit cell (Table 1). An empirical correction for X-ray absorption was made using the program SADABS (part of the Bruker program SAINT). Equivalent reflections were merged into a set of 260 independent reflections ($R_{int} = 0.017$), out of which 238 ones had $I_{obs} > 2\sigma(I_{obs})$ and were used for the structure analysis and refinements.

The initial structure model of $Ti_3(Si_{0.43}Ge_{0.57})C_2$ was taken from that reported for Ti_3SiC_2 [5], which has the space group $P6_3/mmc$ (#194). The structure refinements were performed with the program SHELX97. All atoms were refined with anisotropic thermal displacement parameters, by assuming the ideal composition of $Ti_3(Si_{0.5}Ge_{0.5})C_2$, with Ti at the two M sites (M1 and M2), (Si + Ge) at the A site, and C at the X site. After the convergence of the refinement, which yielded the R_1 factor of 0.014, atomic occupancies for all four sites were allowed to vary. The results showed that, within the experimental uncertainties, the M (both M1 and M2) and X sites were fully occupied by Ti and C, respectively, but the atomic occupancies at the A site deviated slightly from the starting composition (0.5Si + 0.5Ge). Thus, in the subsequent refinements, the atomic occupancies at M and X sites were fixed to the ideal values and only those at the A site were refined with the constraint of (Si + Ge) = 1, yielding Si = 0.4284(2) and Ge = 0.5716(2), with the R_1 factor of 0.010 for the observed reflections and 0.013 for all independent reflections. Final atomic coordinates and anisotropic thermal displacement parameters are listed in Table 2 and selected bond distances and angles in Table 3.

Table 1
Summary of crystal data and refinement results

Structural formula	$Ti_3(Si_{0.43}Ge_{0.57})C_2$
Formula weight	218.06
Crystal size (mm^3)	$0.08 \times 0.07 \times 0.06$
Data collection condition	Room temperature
Space group	$P6_3/mmc$ (no. 194)
a (Å)	3.0823(1)
c (Å)	17.7702(6)
V ($Å^3$)	146.21(1)
Z	2
ρ_{calc} (g/cm^3)	4.953
λ (Å)	0.71069
μ (mm^{-1})	12.92
θ range for data collection	0 to 43
No. of reflections collected	3180
No. of independent reflections	260
No. of reflections with $I > 2\sigma(I)$	238
No. of parameters refined	13
R (int)	0.017
Final R factors ($I > 2\sigma(I)$)	$R_1 = 0.010$, $wR_2 = 0.022$
Final R factors (all data)	$R_1 = 0.013$, $wR_2 = 0.025$
Goodness-of-fit	1.325

Table 2
Atomic coordinates and anisotropic displacement parameters for $Ti_3(Si_{0.43}Ge_{0.57})C_2$

Atom	X	y	z	U_{11}	U_{33}	Ueq
Ti1	0	0	0	0.00327(8) [0.001(1)	0.00337(9) 0.007(2)	0.00331(6) 0.0029(9)]
Ti2	1/3	2/3	0.13410(1) [0.3148(2)	0.00355(7) 0.0029(9)	0.00393(7) 0.013(2)	0.00367(6) 0.0057(6)]
A	0	0	1/4	0.00965(11) [0.009(1)	0.00376(10) 0.01(2)	0.00768(8) 0.0080(6)]
C	1/3	2/3	0.57199(6) [0.5723(1)	0.00409(27) 0.0014(4)	0.00444(33) 0.0092(9)	0.00420(18) 0.0038(3)]

Note: A = Si + Ge; $U_{22} = U_{11}$; $U_{12} = 0.5U_{11}$; $U_{13} = U_{23} = 0$. The data in square brackets are taken from Barsoum et al. [6] for comparison.

Table 3
Selected bond distances (Å) and angles (°)in $Ti_3(Si_{0.43}Ge_{0.57})C_2$

	$Ti_3(Si_{0.43}Ge_{0.57})C_2$ [this work]	Ti_3SiC_2 [5]	Ti_3SiC_2 [6]
C–Ti1 (× 3)	2.1916(7)	2.176	2.181(1)
C–Ti2 (× 3)	2.0941(6)	2.088	2.083(2)
C–Ti (mean)	2.1429	2.132	2.132
Oct. vol. ($Å^3$)	13.071	12.889	12.875
OAV	8.837	6.452	8.709
Ti1–C–Ti1	89.37(3)	89.26	89.30
Ti1–C–Ti2	87.86(1)	88.25	87.90
Ti2–C–Ti2	94.78(4)	94.12	94.76
A–Ti2 (× 6)	2.7219(2)	2.681	2.693(2)
A–A	3.082	3.058	3.066
Ti1–Ti2	2.9741(2)	2.970	2.960

Note: A = Si + Ge; OVA—octahedral angle variance [13].

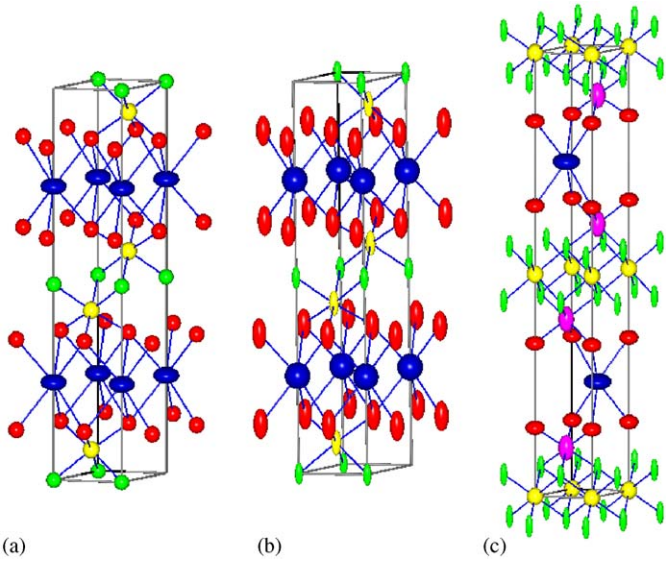

Fig. 1. Crystal structures of MAX phases: (a) $Ti_3(Si_{0.43}Ge_{0.57})C_2$, (b) Ti_3SiC_2 [6], and (c), Ti_4AlN_3 [7]. Thermal ellipsoids are drawn with 99% probability. In all figures, green and red ellipsoids represent Ti1 and Ti2 atoms, respectively, blue ellipsoids, (Si + Ge) or Al, and yellow and pink ellipsoids C or N.

3. Results and discussion

The basic structural features of $Ti_3(Si_{0.43}Ge_{0.57})C_2$ are consistent with those reported for Ti_3SiC_2 [5,6] in terms of bond lengths and bond angles from powder X-ray and neutron diffraction analyses (Table 3). However, a detailed examination of the structural data reveals a significant discrepancy in atomic displacement parameters between our and previous studies (Fig. 1). Specifically, in our study, all Ti (both Ti1 and Ti2) and C atoms display relatively isotropic displacements, whereas A (= 0.43Si + 0.57Ge) exhibits a noticeable displacement anisotropy, with $U_{11} = U_{22} = 0.0097(1)\,Å^2$ and $U_{33} = 0.0038(1)\,Å^2$. In contrast, Barsoum et al. [6] found that the thermal vibrations of Si in Ti_3SiC_2 are quite isotropic at 27, 531 and 714 °C, but anisotropic at 355 and 906 °C. Vibrations of the other atoms are considerably greater along the *c*-axis than along *a*, but the ratio of these amplitudes varies appreciably at various temperatures. Such inconsistency in atomic displacement parameters is likely a reflection of the difficulty in obtaining meaningful anisotropic displacement parameters from powder diffraction data for samples showing strong preferred orientation. As noted by Barsoum et al. [6], layered MAX phases exhibit preferred orientation in powder X-ray and neutron diffraction, but attempts to include the preferred orientation factor into their structure model did not improve the fits significantly to the experimental data and sometimes resulted in negative atomic displacement parameters. Kisi et al. [5] also refined the structure of Ti_3SiC_2 with neutron powder diffraction data, but no detailed information for atomic anisotropic displacement parameters was given, due probably to the fact that their attempt to refine the anisotropic displacement parameters for Si yielded $\beta_{11} \approx 0.045$ and $\beta_{33} \approx 0$ and the error estimates for other atoms were large. Using X-ray and neutron powder diffraction data, Rawn et al. [7] refined the structure of an MAX phase with the composition of Ti_4AlN_3 by including the March–Dollase preferred orientation correction. Although the displacement ellipsoid of Al in this compound is rather anisotropic and has a similar aspect ratio as that of (Si + Ge) in our sample, the displacement ellipsoids for N and Ti atoms do not appear to be consistent with each other (Fig. 1(c)).

A TLS (translation/libration/screw) rigid-body analysis [11,12] of the CTi_6 group reveals that the amplitudes of vibration of C towards Ti are approximately equal to the amplitude of vibration of Ti towards C, with the difference in mean-square displacement amplitudes, $\Delta_{CTi} = 0.00072\,Å^2$. This value indicates that the C–Ti bonds behave like rigid rods, vibrating in tandem. The Ti–Ti contacts along the edges of the octahedra are even more rigid, with $\Delta_{TiTi} = 0.00026\,Å^2$. Together, this implies that the CTi_6 octahedra behave as rigid units, vibrating and oscillating in tandem. Very little of the motion can be attributed to libration (no librational component to the rigid-body motion was revealed by the TLS analysis), while most is translation, as one would, expect when the octahedral form a closely packed sheet. As such, no bond-length correction due to thermal motion was applied to the C–Ti bond lengths. A similar analysis of the A–Ti groups shows no indication of rigid bond behavior, with $\Delta_{ATi} = 0.00251\,Å^2$. The refined displacement parameters therefore indicate that the octahedral sheets are strong units that oscillate back and forth under translational components of thermal motion, while the A cations are more loosely bound, with a motion independent of the others. All atoms appear to vibrate with similar amplitudes parallel to the *c*-axis, ~0.062 Å.

Based on neutron powder diffraction data collected between 25 and 1000 °C, Barsoum et al. [6] observed a dramatic change in the displacement ellipsoid of Si, which is

relatively isotropic at 714 °C, but becomes considerably anisotropic at 906 °C, with the displacements preferentially in the *a–b* plane ($U_{11} = U_{22} = 0.038\,\text{Å}^2$ and $U_{33} = 0.025\,\text{Å}^2$). Although the real cause for this change is unclear, Barsoum et al. [6] suggested that the strong vibrations of Si within the *a–b* plane at 906 °C could be a potential contributing factor to the surprisingly small thermal expansion anisotropy they observed for Ti_3SiC_2 ($\alpha_a = 8.63 \times 10^{-6}$ and $\alpha_c = 9.75 \times 10^{-6}$). Nevertheless, if our room-temperature data on atomic displacement parameters are used for comparison with the high-temperature data measured by Barsoum at al. [6], then the dramatic change reported by Barsoum et al. [6] in the Si displacement parameters as a function of temperature may not be real.

Due to the size difference between Si and Ge, the substitution of Ge for Si results in an increase in the A–Ti bond distances (Table 3). The difference in nearest neighbor bond lengths between Si metal and Ge metal is 0.098 Å. Therefore, substitution of 57% Ge for Si is consistent with an increase of $0.57 \times 0.098 = 0.056$ Å, or an increase of $0.056/2 = 0.028$ Å/A cation. The difference in A–Ti bond lengths between the Si end member and our mixed Ge/Si phase is 0.025 Å, as should be expected based only on substitution. Concurrently, all C–Ti bond lengths increase and the CTi_6 octahedral volume increases from $\sim$12.88 Å^3 in Ti_3SiC_2 to 13.07 Å^3 in $Ti_3(Si_{0.43}Ge_{0.57})C_2$. Nonetheless, no significant change in the CTi_6 octahedral distortions is observed, as measured by the octahedral angle variance and quadratic elongation [13] (Table 3).

Kisi et al. [5] noted that the average C–Ti distance (2.132 Å) in the CTi_6 octahedron in Ti_3SiC_2 is the same as the ideal covalent bond length between Ti^{IV} (1.36 Å) and C^{IV} (0.77 Å), but slightly shorter than that (2.164 Å) in TiC [14]. They further suggested that the relatively shorter C–Ti distance in Ti_3SiC_2 might provide additional screening for its good electrical conductivity, which is a factor of three higher than that [$(1.6 \times 10^6\,(\Omega\text{m})^{-1})$] reported for TiC [15]. Although the average C–Ti bond length (2.143 Å) in our material is slightly longer than that in Ti_3SiC_2, it would be unwise to make a direct link between the structure information and electrical conductivity without further experimental data. On the other hand, the A–Ti distance (2.722 Å) in $Ti_3(Si_{0.43}Ge_{0.57})C_2$ is significantly greater than the ideal covalent bond value (2.56 Å) or the sum of metallic Ti and covalent (0.43Si + 0.57Ge) radii (2.65 Å). Nonetheless, among all atoms in the structure, the A atom exhibits the largest U_{eq} and markedly anisotropic displacements, which may arise from the disordering of Si and Ge at the A site or/and suggest the weak bonding between A and its neighbor atoms.

A procrystal electron density analysis was conducted on the refined structure of $Ti_3(Si_{0.43}Ge_{0.57})C_2$ to investigate the bonding distribution around the A-site atoms. In the procrystal model, static, ground state atomic electron density functions are centered at the observed positions of the atoms. The electron density at a given point in the crystal is the linear sum of the contributions from each of the atoms [16]. In a series of ground-breaking papers on the analysis of the electron density distribution, Bader and coworkers [17–20] showed that a bond exists between a pair of atoms only if a bond-critical point is found along an associated bond path. The bond path is a ridge or line of electron density that is a maximum in a perpendicular plane, and the bond critical point is the minimum point along the bond path where the gradient is zero. If both features are found, then the atoms can be considered as bonded. Downs et al. [16] showed that the procrystal model is capable of reproducing all bond critical points found from full ab initio quantum calculations.

The procrystal analysis was performed with the SPEEDEN program [21] and confirmed that C is bonded to 6Ti atoms and that one Ti1 is bonded to 6C while the other, Ti2, is bonded to 3C and 3A atoms, as expected from the distribution of bond lengths. Furthermore, the analysis showed there is a critical point about halfway between two A atoms, with electron density, $\rho(r_c) = 0.1908\,\text{e/Å}^3$, and Laplacian, $\nabla^2\rho(r_c) = 0.68\,\text{e/Å}^5$. In constrast, the bond critical point between Ti and A exhibits $\rho(r_c) = 0.2247\,\text{e/Å}^3$, and Laplacian, $\nabla^2\rho(r_c) = 1.41\,\text{e/Å}^5$. The results indicate that each A atom is bonded to 6Ti atoms as well as to its 6 nearest neighbor A site atoms, whether the site is occupied by Si or Ge. A contour plot of the electron density distribution in the *a–b* plane through A atoms is shown in Fig. 2. According to Bader [17], the value of the Laplacian can be used to indicate the nature of the bond and the typical Laplacian values for oxide bonds are found to range from $-15 < \nabla^2\rho(r_c) < 30$ [16]. As the A–A and A–Ti bonds display similar bond-critical-point properties, these two bonds may have some similarities in the nature.

It should be pointed out that the bonding between Si atoms in Ti_3SiC_2 has been considered from the

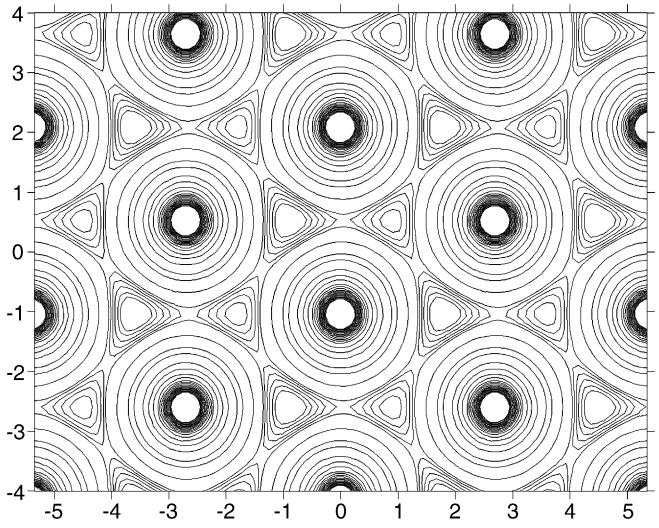

Fig. 2. A contour map of the procrystal electron density distribution through the plane with $z = 0.25$ in $Ti_3(Si_{0.43}Ge_{0.57})C_2$. The contours presented are between 0 and 10 e/Å^3. The unit of numbers on the horizontal and vertical axes is in Angstrom. Note the six bond paths around each Si/Ge atom. These bond paths indicate Si–Si bonds and may provide conduits for electron transfer.

full-potential linear-muffin-tin-orbital (FLMTO) calculations [22], which shows that Si–Si atoms form a covalent bond network within the Si monolayers as a result of the interaction from the hybridization of Si3*p*–Si3*p* states. Nevertheless, Barsoum [1] argued that the presence of Si–Si bonds in Ti_3SiC_2 is highly unlikely because the Si–Si distance in elemental Si (2.3532 Å) is considerably shorter than here (3.0656 Å).

Bond strength is correlated with the value of the electron density at the critical point. The value of $\rho(r_c)$ for the Ti–C bond is 0.440 e/Å^3, indicating the following bond-strength order in $Ti_3(Si_{0.43}Ge_{0.57})C_2$: Ti–C ≫ Ti–A > A–A. This, of course, is obvious by the bond length distribution, and is consistent with the rigid-body analysis discussed above.

Most importantly, the bond paths between the A-site atoms suggest that these paths may be significantly involved with electron transport. Gibbs et al. [23] recently found Ni–Ni bond paths in nickel sulfides and correlated them to electrical conductive properties. The Si–Si and Ge–Ge interactions have no potential difference across the length of the bond, so if these bond paths can be maintained, then the resistance to electron conductivity is lowered. Gibbs et al. [23] likened the distribution of bond paths to a system wired with atomic scale paths. Thus the A–A interactions in the MAX phases may provide additional contribution to the electrical conductivity in the directions along the *a*–*b* plane.

References

[1] M.W. Barsoum, Prog. Solid State Chem. 28 (2000) 201.
[2] M.W. Barsoum, T. El-Raghy, J. Am. Ceram. Soc. 79 (1996) 1953.
[3] W. Jeitschko, H. Nowotny, F. Benesovsky, Monatsh. Chem. 94 (1963) 1198.
[4] W. Jeitschko, H. Nowotny, Monatsh. Chem. 98 (1967) 329.
[5] E.H. Kisi, J.A.A. Crossley, S. Myhra, M.W. Barsoum, J. Phys. Chem. Solids 59 (1998) 1437.
[6] M.W. Barsoum, T. El-Raghy, C.J. Rawn, W.D. Porter, H. Wang, E.A. Payzant, C.R. Hubbard, J. Phys. Chem. Solids 60 (1999) 429.
[7] C.J. Rawn, M.W. Barsoum, T. El-Raghy, A. Procopio, C.M. Hoffmann, C.R. Hubbard, Mater. Res. Bull. 35 (2000) 1785.
[8] M.W. Barsoum, C.J. Rawn, T. El-Raghy, A.T. Procopio, W.D. Porter, H. Wang, C.R. Hubbard, J. Appl. Phys. 87 (2000) 8407.
[9] A. Ganguly, T. Zhen, M.W. Barsoum, J. Alloys Compounds 376 (2004) 287.
[10] B. Manoun, H.P. Liermann, R. Gulve, S.K. Saxena, A. Ganguly, M.W. Barsoum, C.S. Zha, Appl. Phys. Lett. 84 (2004) 2799.
[11] V. Schomaker, K.N. Trueblood, Acta Crystallogr. B 24 (1968) 63.
[12] R.T. Downs, High-temperature and high-pressure crystal chemistry, in: R.M. Hazen, R.T. Downs (Eds.), Reviews in Mineralogy and Geochemistry, Mineralogy Society of America, Washington, DC, 2000, pp. 41–61.
[13] K. Robinson, G.V. Gibbs, P.H. Ribbe, Science 172 (1971) 567.
[14] A.N. Christensen, Acta Chem. Scand. Ser. A 32 (1978) 89.
[15] W.S. Willams, Phys. Rev. A. 135 (1964) 505.
[16] R.T. Downs, G.V. Gibbs, M.B. Boisen Jr., K.M. Rosso, Phys. Chem. Minerals 29 (2002) 369.
[17] R.F.W. Bader, Atoms in Molecules, Oxford Science Publications, Oxford, UK, 1990.
[18] R.F.W. Bader, J. Phys. Chem. A 102 (1998) 7314.
[19] J. Hernandez-Trujillo, R.F.W. Bader, J. Phys. Chem. A 104 (8) (2000) 1779.
[20] R.F.W. Bader, C.F. Matta, Organometallics 23 (2004) 6253.
[21] R.T. Downs, A. Andalman, M. Hudasko, Am. Mineral. 81 (1996) 1344.
[22] N.I. Medvedeva, D.L. Novikov, A.L. Ivanovsky, M.V. Kuznetsov, A.J. Freeman, Phys. Rev. B 58 (1998) 16042.
[23] G.V. Gibbs, R.T. Downs, C.T. Prewitt, K.M. Rosso, N.L. Ross, D.F. Cox, J. Phys. Chem. B 109 (2005) 21788.